Multiple Quantum ^{27}Al Magic-Angle-Spinning Nuclear Magnetic Resonance Spectroscopic Study of $SrAl_{12}O_{19}$: Identification of a ^{27}Al Resonance from a Well-Defined AlO_5 Site

Stephan R. Jansen,† Hubertus T. Hintzen,* and Ruud Metselaar

Laboratory of Solid State and Materials Chemistry, Centre for Technical Ceramics, Eindhoven University of Technology, P.O. Box 513, 5600 MB Eindhoven, The Netherlands

Jan W. de Haan and Leo J. M. van de Ven

Laboratory of Instrumental Analysis, Eindhoven University of Technology, P.O. Box 513, 5600 MB Eindhoven, The Netherlands

Arno P. M. Kentgens* and Gerda H. Nachtegaal

SON/NWO HF-NMR Facility, NSR Center, University of Nijmegen, Toernooiveld 1, 6525 ED Nijmegen, The Netherlands

Received: February 20, 1998; In Final Form: May 1, 1998

$SrAl_{12}O_{19}$, a material with the magnetoplumbite-type structure, has been characterized by field-dependent ^{27}Al MAS and MQMAS solid-state NMR. In this material five different Al sites are present: one AlO_4, one AlO_5, and three AlO_6 sites, which all could be revealed by a quintuple quantum (5Q) MAS spectrum recorded at 7.05 T. A distribution is measured in the NMR parameters that is ascribed to statistical disorder of aluminum in the AlO_5 polyhedron. Quantitative simulations, using distributions in quadrupole coupling constant (C_q), of the conventional MAS spectra were successful in fitting the spectra. The ^{27}Al resonance of the AlO_5 polyhedron has a relatively high shielding (δ_{iso}: 18 ppm) and a C_q of 2.1 MHz. The high shielding is explained by the distortion of the 5-fold-coordinated Al because a relation seems to exist between the isotropic chemical shift and the distortion of 5-fold-coordinated aluminum in various materials.

Introduction

Solid-state NMR is becoming increasingly important in solving structural problems of various materials. Recently, we were able to distinguish between related aluminates with a magnetoplumbite- or β-alumina-type structure using the ratio of the ^{27}Al NMR signals of tetrahedral and octahedral Al.[1] As is already known on the basis of structural data obtained by X-ray diffraction,[2] besides the ratio between the tetrahedral/octahedral Al sites another difference between these two structural types exists: the presence of an AlO_5 site in aluminates with the magnetoplumbite-type structure (Figure 1). So far however, this 5-fold coordinated Al site has not been identified by NMR.[1] At this moment no literature data are known dealing with the ^{27}Al NMR signal of the AlO_5 polyhedron in magnetoplumbite-type materials, although some NMR data concerning aluminates with the magnetoplumbite-type structure were published.[4,5]

An important characteristic of ^{27}Al solid-state NMR is the dependence of the isotropic chemical shift (δ_{iso}) of the central transition ($+^1/_2$, $-^1/_2$) resonance on local Al coordination: AlO_4 (∼80−45 ppm) and AlO_6 (∼20 to −20 ppm).[6] For each coordination the ranges in the isotropic chemical shift (shielding) are found to correlate with the chemical composition of the second coordination sphere (the so-called next nearest neighbors) and the bond angles between the aluminum ions, and ions from the first and the second coordination sphere. Usually the range of ∼40−25 ppm is taken to identify the AlO_5 polyhedra.[6] But as becomes clear from the Table 1, the range of experimental values is much wider (∼52−14 ppm), resulting in an overlap with the signals of AlO_4 as well as AlO_6 polyhedra, thus hindering unambiguous assignments of the signals. Furthermore, there is a wide spread in quadrupole coupling constant (C_q ∼ 1−11 MHz) and asymmetry parameter (η). These broad ranges in C_q and η are caused by the large variety in symmetries

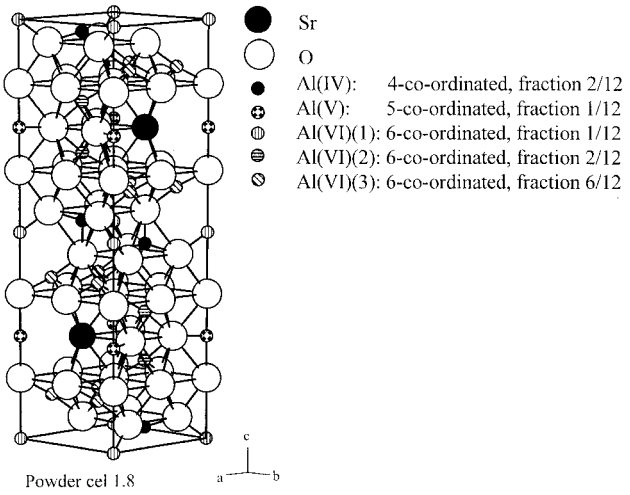

Figure 1. Unit cell of $SrAl_{12}O_{19}$ (space group $P6_3/mmc$), after ref 3. The various Al sites are shown in this figure, together with the coordination and the multiplicity of these sites.

† Present address: Philips Lighting B.V., P.O. Box 80020, 5600 JM Eindhoven, The Netherlands.

* To whom correspondence should be addressed. E-mail H. T. Hintzen: tgtvbh@chem.tue.nl. E-mail A. P. M. Kentgens: arno@solidmr.kun.nl.

S1089-5647(98)01224-3 CCC: $15.00
Published on Web 07/10/1998

TABLE 1: NMR Characteristics (Isotropic Chemical Shift, δ_{iso}, Quadrupole Coupling Constant, C_q, and Asymmetry Parameter, η) of Several 5-Fold Coordinated Al Nuclei

name	chemical composition	ref	δ_{iso} [ppm]	C_q [MHz]	η	no. of AlO_5 sites
andulasite	Al_2SiO_5	7	35	5.73	0.7	1
neodymium aluminum digermanate	$NdAlGe_2O_7$	8	35	7.2	0.3	1
dialuminum digermanate	$Al_2Ge_2O_7$	8	36	8.8	0.4	1
AlPO-21	Al_3PO_4-21	9	14	5.1	0.4	2
			16	7.4	0.65	
AlPO-21	Al_3PO_4-21	10	14.6	5.9	0.68	2
			15.7	7.4	0.52	
grandiderite	$Mg_{0.9}Fe_{0.1}Al_3SiBO_9$	11	41	8.7	0.95	1
senegalite	$Al_2(OH)_3PO_4.H_2O$	12	36	2.87	0	1
augelite	$Al_2PO_4(OH)_3$	12	30.9	5.7	0.85	1
vesuvianite	$Ca_{10}Al_4(Mg,Fe)_2Si_9O_{34}(OH)_4$	13	41.1	nd[a]	nd	1
barium aluminum glycolate	$Ba[Al_2(C_2H_4O_2)_4]$	14	35.3	4	nd	1
"pyrophyllite dehydroxylate"	$Al_2Si_4O_{11}$	15	29	10.5	0.6	1
aluminum borate	$Al_{18}B_4O_{33}$	16	43	1.42	0.490	2
			52	1.08		
aluminum borate	$Al_{18}B_4O_{33}$	17	44	1.191	0.7	2
			52	1.016	0.06	

[a] nd: not determined.

of the AlO_5 polyhedra. So it can be concluded that due to the influence of the chemical composition of the second coordination sphere and the insufficient amount of NMR data concerning AlO_5 polyhedra, no unambiguous criteria can be defined concerning the assignment of NMR parameters for 5-fold-coordinated Al.

A problem of MAS NMR spectra of half-integer quadrupolar nuclei like Al ($I = 5/2$) is their limited resolution. It is well-known that MAS averages dipolar interactions and chemical shift anisotropies but is not capable of averaging second-order quadrupole effects. As a result MAS spectra show an apparent shift and broadening of the lines. To overcome these problems, new averaging schemes, double-rotation (DOR),[18] dynamic-angle spinning (DAS),[19,20] and, recently, multiple quantum MAS (MQMAS) NMR were introduced.[21] Since MQMAS is technically less involved than DOR and DAS and are obtained using standard MAS probe-heads, it was soon picked up by various research groups. The basic idea of this experiment is to refocus second-order quadrupolar broadenings in MAS NMR spectra by creating echoes of multiple-quantum transitions and the directly observable central transition of a half-integer spin system. As has been discussed, the central $\langle +1/2| \leftrightarrow |-1/2\rangle$ transition is broadened in second-order by the quadrupolar interactions, and the angular dependence of this interaction contains fourth-rank terms that are not cancelled by MAS. This appears to be true for every $\langle +m| \leftrightarrow |-m\rangle$ multiple-quantum transition. Frydman and Harwood[21] realized that the angular dependencies of these multiple-quantum transitions have a form similar to that of the central transition but with different zero-, second-, and fourth-rank coefficients. Under MAS, the second-rank terms are averaged. Thus the frequency spectrum of a $\langle +m| \leftrightarrow |-m\rangle$ transition has the same (but scaled) shape as the central $\langle +1/2| \leftrightarrow |-1/2\rangle$ transition. Although multiple-quantum transitions cannot be detected directly by acquisition, they can be detected indirectly in a two-dimensional experiment consisting of an excitation pulse, an evolution period, and a conversion pulse followed by the detection period. The first pulse excites many transitions in the quadrupolar spin system, and therefore its phase is cycled in such a way to pick out the desired multiple-quantum coherence. The second pulse converts $2m$-quantum coherence to single-quantum coherence, and the normal central transition signal is acquired. Two-dimensional Fourier transformation of these signals leads to a spectrum with the resonances located at

$$\nu_1 = 2m\nu_{iso} + C_0(I,m)\nu_{QIS} + C_4(I,m)\, P_4(\cos(\theta_m))\, \nu_4(\alpha,\beta)$$
$$\nu_2 = \nu_{iso} + C_0(I,1/2)\nu_{QIS} + C_4(I,1/2)\, P_4(\cos(\theta_m))\, \nu_4(\alpha,\beta) \quad (1)$$

where ν_{iso} is the isotropic chemical shift, ν_{QIS} is the quadrupole-induced shift, and $\nu_4(\alpha,\beta)$ is the fourth-order angular dependence responsible for the second-order line broadening. At the magic angle the fourth-order Legendre polynomial $P_4(\cos(\theta_m)) = -7/18$. The C's are constants depending on the quantum numbers I and m.[21,22] The resulting two-dimensional spectrum will be free of anisotropic quadrupolar broadenings along the line $\nu_1 = (C_4(I,m)/C_4(I,1/2))\nu_2$.

In view of the efficiency of the excitation and conversion pulses, generally the triple-quantum coherence is chosen. In cases where sensitivity is not a problem, but resolution is still limited with several resonances in a small chemical shift range, it is interesting to look at higher order transitions,[23] as the spread in chemical shift (in Hz) is multiplied by the order of the transition. In the present contribution we had to resort to 5Q MAS experiments (5/2, −5/2 transition) to completely resolve the spectrum of $SrAl_{12}O_{19}$.

In this paper, we discuss the results of our investigation of the ^{27}Al NMR parameters characteristic for the five Al sites in $SrAl_{12}O_{19}$ with the magnetoplumbite-type structure, with emphasis on the data for the AlO_5 polyhedron. For this purpose we have performed conventional ^{27}Al MAS NMR at various magnetic field strengths as well as triple- and quintuple-quantum ^{27}Al MAS NMR experiments.

Experimental Section

Sample Preparation and Characterization. The starting mixture was made by combining the appropriate amounts of $SrCO_3$ (Riedel-de Haen AG, >99%) and γ-Al_2O_3 (Sumitomo AKPG, >99.995%). Corrections were made for weight losses. The choice of this type of Al_2O_3 powder as a starting material is based on its high reactivity.[24] The starting mixture was wet-mixed in 2-propanol (>97%) for 2 h in an agate container with agate balls on a planetary mill. After mixing, the 2-propanol

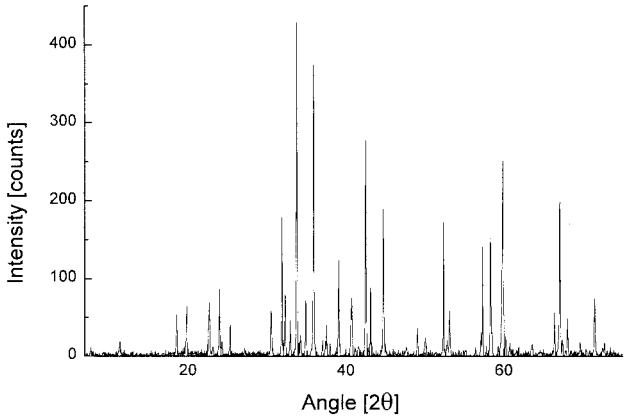

Figure 2. X-ray diffraction pattern for single-phase crystalline $SrAl_{12}O_{19}$ fired at 1973 K.

was evaporated. The powder was dried in a stove for one night at 433 K, and it was subsequently ground in an agate mortar.

The powder was fired in a molybdenum crucible under a mildly flowing N_2/H_2 (90/10) gas mixture. Reactions were performed in a vertical high-temperature tube furnace at 1973 K for 2 h. Heating and cooling rates of 3 K/min were used.

The phases, present after reaction, were determined by powder X-ray diffraction (XRD). Continuous scans were made with Cu Kα radiation from 5° to 75° (2θ), with a scan speed of 1° (2θ)/min (Philips 5100). The lattice parameters were calculated by using the following reflections: 2 0 14, 2 2 0, 2 0 13, 3 0 4, 2 0 11, 2 1 7, 1 0 11, 1 1 8, 2 0 6, 2 0 5, and 1 0 10.

NMR Spectroscopy. Conventional MAS NMR spectra were obtained by single pulse excitation on the following spectrometers: (1) a Bruker DPX 200 (4.7 T) spectrometer equipped with a Bruker BB CP-MAS 4 mm double-tuned probe, operating at 52.15 MHz, rf-field = 80 kHz, pulse-length = 0.7 μs, and magic angle spinning at 13.65 kHz; (2) a Bruker DMX 300 (7.1 T) equipped with a Bruker BB CP-MAS 4 mm double-tuned probe, operating at 78.21 MHz, rf-field = 80 kHz, pulse-length = 2.1 μs, and magic angle spinning at 12.1 kHz; using these conditions, also a satellite transition spectroscopy (SATRAS) spectrum was recorded; (3) a Bruker MSL 400 (9.4 T) NMR spectrometer equipped with a Standard Bruker double air-bearing 4 mm MAS probe-head, operating at 104.56 MHz, rf-field = 110 kHz, pulse-length = 1 μs, and magic angle spinning at 15 kHz; (4) a Bruker AMX 600 (14.1 T) NMR spectrometer equipped with a home-built single-tuned MAS probe-head fitted with a Jakobsen 5 mm MAS assembly, operating at 152.38 MHz, rf-field = 70 kHz, pulse-length = 0.6 μs, and magic angle spinning at 13.3 kHz.

At 4.7 and 14.1 T pulses were chosen short enough to ensure quantitative analysis of the conventional MAS data.

The 5Q-MAS spectrum was recorded using the two-pulse sequence[22] completed with a z-filter using a selective $\pi/2$ pulse as described by Amoureux et al.[25] The experiment was performed in a 4 mm Bruker MAS probe, using an rf-field strength of 90 kHz for the excitation and conversion pulses and 15 kHz for the selective pulse. Phase cycling of four times 10 phases was employed to select the quintuple-quantum coherence during the evolution period. TPPI was used to achieve quadrature detection in t_1. The spinning speed was 12.1 kHz.

Results and Discussion

XRD Characterization. The XRD measurement confirmed (Figure 2) that after firing at 1973 K the material is single-phase $SrAl_{12}O_{19}$ with the magnetoplumbite-type structure. The crystallographic data, which are in agreement with literature data,[2,3] are shown in Table 2.

TABLE 2: Lattice Parameters (from this Work and Literature) of $SrAl_{12}O_{19}$ with the Magnetoplumbite-Type Structure, after Firing at 1973 K

unit cell dimensions (SD)	system: hexagonal	space group: $P6_3/mmc$ (194)
this work	$a = 5.567(1)$ [Å]	$c = 22.002(2)$ [Å]
	$c/a = 3.952(1)$	$V = 590.6(2)$ [Å^3]
ref 2	$a = 5.5666(2)$ [Å]	$c = 22.0018(8)$ [Å]
	$c/a = 3.9525(2)$	
ref 3	$a = 5.562(2)$ [Å]	$c = 21.972(5)$ [Å]
	$c/a = 3.950(2)$	

Determination of NMR Parameters. Figure 3 shows the conventional MAS spectra obtained at four different magnetic fields. Although the quadrupolar broadening is smallest at the highest external field, this does not result in a separated AlO_5 signal. On the basis of the signal intensities at the highest field ($I_{50-70\ ppm}/I_{25--10\ ppm} < 0.2$), it is clear that the AlO_5 signal is obscured by the three AlO_6 signals and not by the AlO_4 signal. The Bruker Winfit program[26] was used to model all four MAS spectra using five signals corresponding to the five Al sites. It appeared to be impossible to model all spectra with less than five resonances (corresponding to less than five crystallographic Al sites). Although the simulated spectra correspond quite well with the four measured MAS spectra, no direct evidence is found for the correctness of this model. Therefore some additional experiments were necessary. Satellite transition spectroscopy (SATRAS) spectra were recorded at 7.1 and 9.4 T. It appeared that the resolution of the sidebands in these spectra was insufficient to resolve the expected five signals of the various crystallographic sites. The SATRAS did prove useful, however, to get an estimate for the quadrupole parameters of one of the 6-fold-coordinated sites. The quadrupole coupling constant of the site designated as Al(VI)(1) (Table 3) is too small to lead to substantial quadrupolar broadening of the central transition in any of the obtained MAS spectra. Due to this rather small C_q, the sidebands of the $\langle \pm 3/2| \leftrightarrow |\pm 1/2\rangle$ satellite transitions are very prominent in the SATRAS spectra, allowing a good estimate of the quadrupole parameters. In a further attempt to resolve the signals of the five different crystallographic sites a DOR spectrum was obtained at 9.4 T, again to no avail. The resolution of both the SATRAS and DOR spectra is compromised by small distributions in the NMR parameters of some of the sites, as can be judged from the blurring of some of the quadrupolar features in the MAS spectra.

To resolve ^{27}Al NMR signals with slightly different NMR characteristics, multiple-quantum MAS NMR was used. From 3Q MAS NMR spectra, recorded at 4.7 and 14.1 T, it was not possible to discern all five Al sites. To further increase resolution, a 5Q MAS NMR measurement was performed at 7.05 T, which resulted in a clearly resolved spectrum (Figure 4) showing five distinctive resonances.

Judging from the conventional MAS, SATRAS, and DOR experiments and confirmed by the MQMAS experiments, there are small but distinct distributions in quadrupolar coupling constant. This is unexpected for a crystalline material because these distributions imply variations of the atomic positions in the crystallographic structure. The XRD pattern (Figure 2) clearly shows a well-crystallized phase, indicating that only small structural distributions are expected. Similar distributions in NMR parameters are observed in 3Q MAS of other crystalline materials, like leucite and anorthite, and are ascribed to the disordered arrangement of second-neighbor cations.[27] According to crystallographic data for $SrAl_{12}O_{19}$, there is a disordered

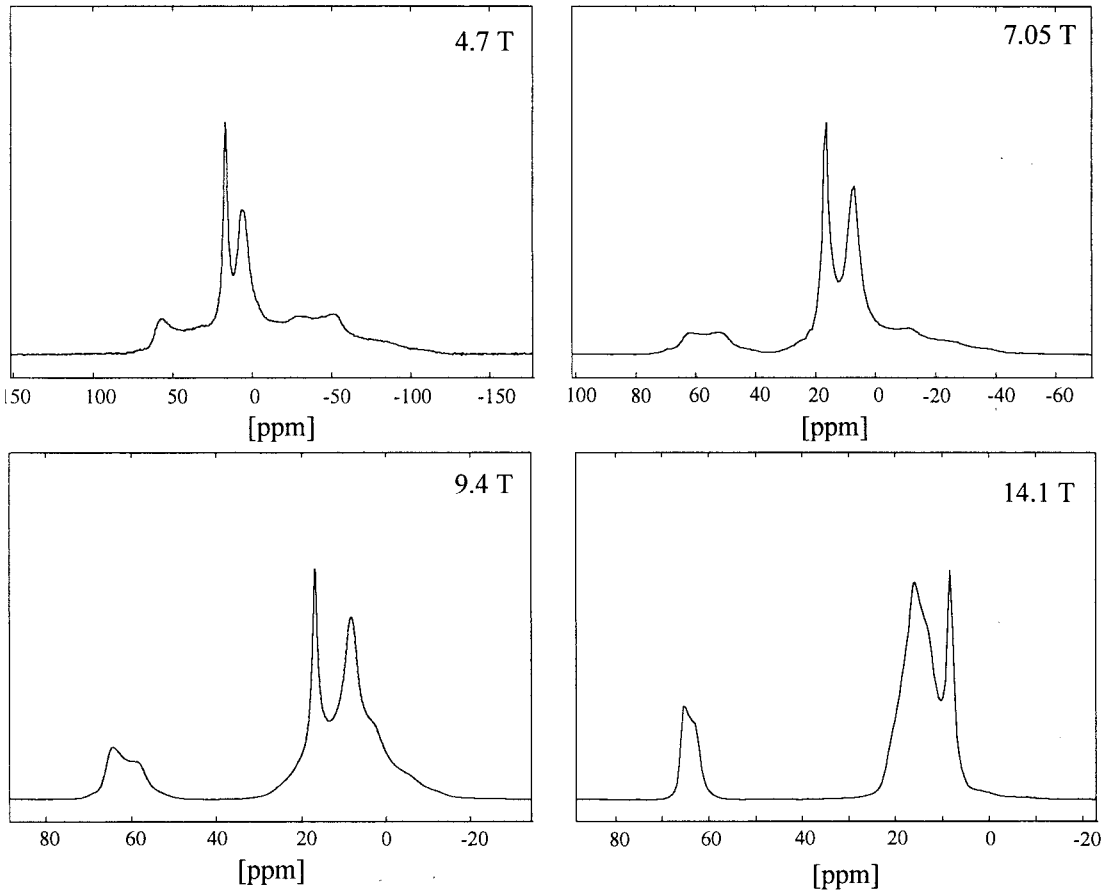

Figure 3. Measured ^{27}Al MAS spectra for $SrAl_{12}O_{19}$ at four different magnetic fields.

TABLE 3: ^{27}Al MAS NMR Parameters and Corrected Intensities (from 4.7 T Spectrum, According to Procedure by Massiot et al.[29]) of $SrAl_{12}O_{19}$ with the Magnetoplumbite-Type Structure. Data in Parentheses are Shown for $CaAl_{12}O_{19}$ with the Magnetoplumbite-Type Structure As Determined by Müller et al.[5]

site	δ_{iso} [ppm]	C_q [MHz]	ΔC_q [MHz]	η	intensity [%]	corrected intensity [%]	expected intensity [%][b]
Al(IV)	68.0 (65)	3.45 (2)	0.15	0.1	16	16.3	16.67
Al(V)	18.0 (nd)[a]	2.1 (nd)	0	0.7	9	8.8	8.33
Al(VI)(1)	17.1 (16)	0.6 (<1)	0	1	17	13.0	8.33
Al(VI)(2)	9.6 (16)	1.3 (<1)	0	1	14	12.9	16.67
Al(VI)(3)	21.7 (9)	4.9 (1.5)	0.11	0.63	44	49.0	50

[a] nd = not determined. [b] On the basis of crystallographic data.

arrangement of the Al(V) atoms.[2] The Al(V) atom is displaced from the site positioned in the so-called mirror plane (Wyckoff letter 2b), thus creating two equivalent sites (Wyckoff letter 4e), which as a consequence are each occupied for only 50% (see Figure 5).[2] A statistical occupation of these sites results in variations of the environments of the other Al ions, thus leading to a distribution of the NMR parameters.

The 5Q MAS spectrum is the only recording that reveals all five signals. However, multiple-quantum MAS NMR is not a quantitative method; that is, the measured fractions of the signal intensities are not equal to the corresponding fractions of the corresponding aluminum ions. Therefore conventional MAS NMR spectra are used for quantitative analysis of the NMR data, as these can be interpreted quantitatively if they are recorded using the appropriate conditions. Starting values of the isotropic chemical shifts and the quadrupolar coupling constants for the five Al sites obtained by 5Q MAS were used for the simulations of the conventional MAS NMR spectra. The asymmetry parameter was optimized using the Bruker Winfit program.[26] To improve the quantitative simulation of the NMR data further, the parameters optimized in this way are used as input in a recently developed program which takes the distribution of the quadrupolar coupling constant into account.[28] Simple Gaussian distributions are used in this case. The distribution of the quadrupolar coupling constants was optimized using the 4.7 T spectrum, as the quadrupolar features are most pronounced at this low field. Simulations using a distribution in the isotropic chemical shift gave no significant improvement of the simulations at various fields and were therefore discarded. The intensities obtained from the refined simulation of the 4.7 T MAS spectrum are tabulated in Table 3. Massiot et al.[29] showed that for MAS spectra the intensity of the centerband, used for quantitative comparisons, has to be corrected depending on the ratio of the spinning speed and the quadrupole frequency. When the spinning speed is relatively slow and/or the quadrupolar interaction is large, the central $\langle +1/2| \leftrightarrow |-1/2\rangle$ transition is split into a sideband pattern which has to be taken into account completely in order to find the correct intensity. In the case of high spinning speeds and small or intermediate quadrupole interactions, however, the centerband contains intensity not only from the central $\langle +1/2| \leftrightarrow |-1/2\rangle$ transition but also varying amounts from the satellite transitions, depending on the value

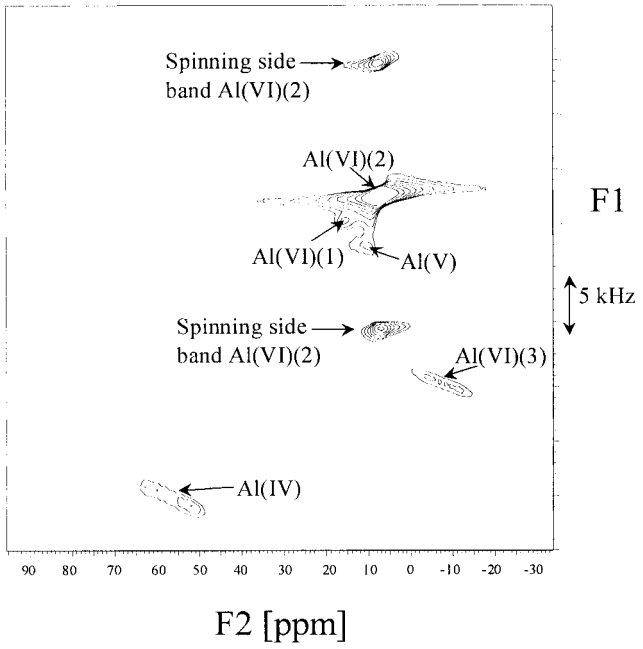

Figure 4. ^{27}Al 5Q MAS spectrum of $SrAl_{12}O_{19}$ at 7.05 T (MAS frequency 12.1 kHz), clearly showing the five Al sites present in this material (numbering according to Figure 1).

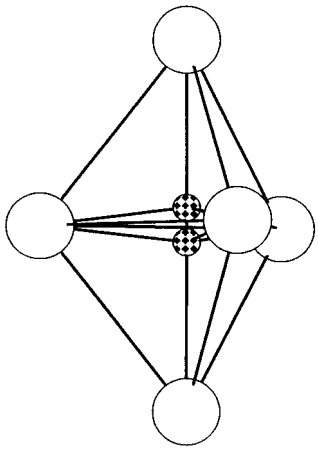

Figure 5. AlO_5 coordination in $SrAl_{12}O_{19}$: a trigonal bipyramid. Both Al(V) positions, above and below the intermediate layer ($z = 0.25$, Figure 1), are shown, but only one of the two is occupied (site occupation of 50%).

of the quadrupolar coupling constant and spinning speed. The latter effect is significant for the Al(VI)1 and Al(VI)2 sites experiencing only a small quadrupolar interaction, whereas the first effect is sizable for the Al(VI)3 site. The appropriate corrections were obtained from Figures 3 and 4 in ref 29. The final set of isotropic chemical shifts, quadrupolar parameters, and asymmetry parameters as well as the intensities (at 4.7 T) of all five Al sites are shown in Table 3. The simulated spectrum at 4.7 T showing the separate resonances as well is shown in Figure 6.

The NMR signal of the Al(IV) site could be straightforwardly assigned on the basis of the isotropic chemical shift. The octahedral sites Al(VI)(1), Al(VI)(2), and Al(VI)(3) could be assigned on the basis of their intensities. Simultaneously, the Al(VI)(1) and Al(V) signal were assigned on the basis of their differences in quadrupolar coupling constant (which is expected to be very small for the Al(VI)(1) site, as there is only a very small distortion of the Al(VI)(1) octahedron).

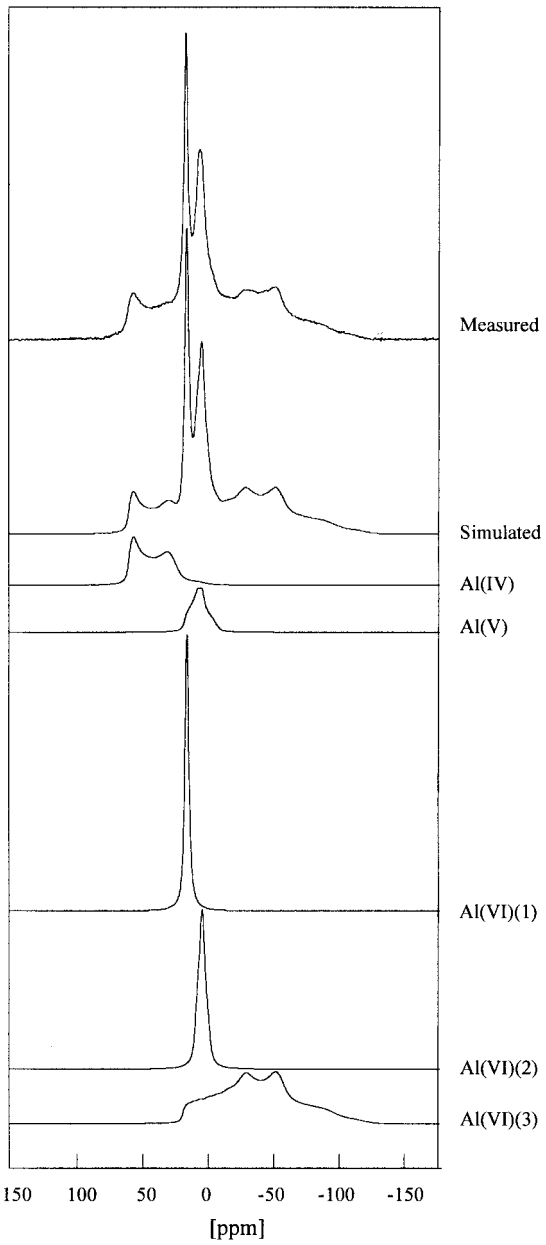

Figure 6. Measured (MAS frequency 13.65 kHz) and simulated ^{27}Al MAS NMR spectrum at 4.7 T and the relative contributions of the various Al sites used to give the simulated spectrum (parameters are shown in Table 3).

The corrected intensities of the NMR signals shown in Table 3 agree very well with the theoretical intensities, except for the Al(VI)(1) and Al(VI)(2) site. These two sites experience relatively small quadrupolar interactions and therefore get the largest intensity corrections. Due to the small C_q values of these sites, their quadrupolar broadenings are not very pronounced in the MAS spectra, and thus there is a relatively large uncertainty in the exact value of C_q as obtained from the lineshape simulations. This subsequently induces a large uncertainty in the correction factors for the intensities obtained from ref 29.

Interpretation of NMR Parameters. In the literature various relationships have been reported between structural and NMR parameters. According to Skibsted et al.[30] the quadrupole coupling constant of tetrahedrally coordinated Al in various aluminates increases with increasing mean bond angle deviation (D) from a perfect tetrahedral symmetry. The mean bond angle deviation is defined by[30]

$$D = \frac{\sum_{i=1}^{i=m} |(\theta_i - \theta_0)|}{m} \quad (2)$$

with θ_i the O−Al−O angles in the AlO_x polyhedron, θ_0 the ideal O−Al−O angle in the polyhedron (109.47° for a tetrahedron), and m the number of angles (6 for a tetrahedron). The quadrupole coupling constant of 3.45 MHz measured for the tetrahedral Al site in $SrAl_{12}O_{19}$ (D = 2.60, derived from crystallographic data[2]) agrees with the value of 3−4 MHz predicted by Skibsted et al. for $CaAl_{12}O_{19}$.[30]

An alternative method to quantify the distortion of a polyhedron is to calculate the tangent of the deviations of the O−Al−O bond angles from those in a perfect polyhedron. This so-called shear strain $|\psi|$ parameter is defined as:[31]

$$|\psi| = \sum_i |\tan(\theta_i - \theta_0)| \quad (3)$$

where θ_i is the O−Al−O angles in the AlO_x polyhedron and θ_0 is the angles in an undistorted polyhedron. Ghose and Tsang found the C_q of Al in AlO_4 tetrahedra in aluminosilicates is highly correlated to the shear strain.[31]

For the Al(IV) site in $SrAl_{12}O_{19}$ a shear strain of 0.27 was calculated from the structure as determined by X-ray diffraction.[2] Its experimental C_q value of 3.45 MHz is in the same range as literature data for tetrahedral Al sites with a comparable shear strain.[31−33] The relatively low isotropic chemical shift, compared to other aluminates (ideally around 80 ppm[34]), can be attributed to the fact that the AlO_4 tetrahedron has neighboring AlO_6 octahedra instead of AlO_4 tetrahedra, as mentioned by Müller et al.[34]

No relationship is observed between the NMR parameters of the AlO_6 octahedra in $SrAl_{12}O_{19}$ and the mean bond angle deviation (D) or the shear strain ($|\psi|$), nor is such a relationship reported in literature for the AlO_6 octahedra in other materials. According to Ghose and Tsang, the quadrupole coupling constant of octahedrally coordinated Al sites increases with increasing longitudinal strain, $|\alpha|$, which is a measure for the variation in Al−O bond lengths and defined by[31]

$$|\alpha| = \sum_i |\ln(l_i/l_0)| \quad (4)$$

where l_i is the individual Al−O bond length and l_0 is the "ideal" bond length of a perfect polyhedron with the same volume as the distorted polyhedron. This relationship between the quadrupole coupling constant and the longitudinal strain also applies to the octahedrally coordinated Al sites in $SrAl_{12}O_{19}$, as is depicted in Figure 7. The longitudinal strain parameters of the octahedral Al sites were calculated from the refined crystal structure data.[2]

When compared to the NMR parameters of 5-fold-coordinated Al sites in other materials (Table 1), it is clear that both the quadrupole coupling constant and the isotropic chemical shift are quite small for the AlO_5 polyhedron in $SrAl_{12}O_{19}$. The AlO_5 polyhedron has an almost ideal trigonal bipyramidal shape with the Al axially displaced from the center,[2] as is depicted in Figure 5. As can be simply calculated, for a trigonal bipyramid the quadrupole coupling constant vanishes when the two axial Al−O bonds are ∼1.1 times longer than the three lateral Al−O bonds. This is not the case in the present system, however. To establish a possible relationship between the NMR parameters and the distortion of the AlO_5 polyhedron, we used the distortion factor

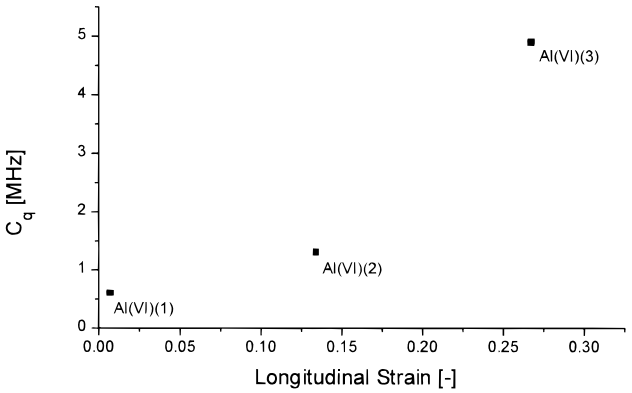

Figure 7. Quadrupolar coupling constant (C_q) vs the longitudinal strain (α, eq 4) for three different sites of octahedrally coordinated Al in $SrAl_{12}O_{19}$.

R as defined by Zemann[35] to quantify this distortion:

$$R = \frac{\sum_{i=1}^{10} |\theta_i - \theta_0|}{\sum_{i=1} \theta_i} \quad (5)$$

Here θ_i is the O−Al−O bond angle of the polyhedron and θ_0 is the ideal O−Al−O bond angle. On the basis of electrostatic energy calculations, Zemann pointed out that the trigonal bipyramid and the tetragonal pyramid are the most favorable configurations for molecular AX_5 complexes and have a remarkably similar energy.[35] Therefore R values of an AlO_5 polyhedron can be calculated with respect to the trigonal bipyramid configuration (θ_0 = 180°, 120° (3×), and 90° (6×)) or the tetragonal pyramid configuration (θ_0 = 151.9° (2×), 104.1° (4×), and 86.6° (4×)[35]) for an ideal AlO_5 polyhedron. The calculated R values of the trigonal bipyramid and the tetragonal pyramid can be compared in an absolute way to discriminate between the two configurations. For all AlO_5 polyhedra mentioned in Table 1, except vesuvianite,[36] the R values calculated with respect to the trigonal bipyramid configuration are smaller than the values calculated with respect to the tetragonal pyramid configuration. This indicates that the polyhedra are closest to the trigonal bipyramid shape, which we therefore use here as the reference AlO_5 configuration. For the AlO_5 polyhedra of the structures given in Table 1, it was not possible to establish a correlation between the distortion parameter R and the quadrupole coupling constant observed in the NMR experiments. Apparently, the distortion of the first (oxygen) coordination sphere has only a minor effect on the quadrupole parameters. Possibly, the arrangement of the next nearest neighbor cations has a stronger effect on the quadrupole parameters, as has been suggested by Smith and Steuernagel for AlO_5 polyhedra.[11] As is seen in Figure 8, a correlation between the isotropic chemical shift and the distortion parameter R is observed. Apparently, the isotropic chemical shift increases with an increasing distortion of the AlO_5 polyhedron. It should be noted, however, that this relationship is based on a limited number of data points, and the correlation is thus not well-substantiated.

From these observations we see that for the AlO_5 polyhedra it is less straightforward to establish a correlation between NMR parameters and structural properties as compared to AlO_4 and AlO_6 polyhedra. For those polyhedra a correlation between isotropic chemical shift and chemical composition of the next

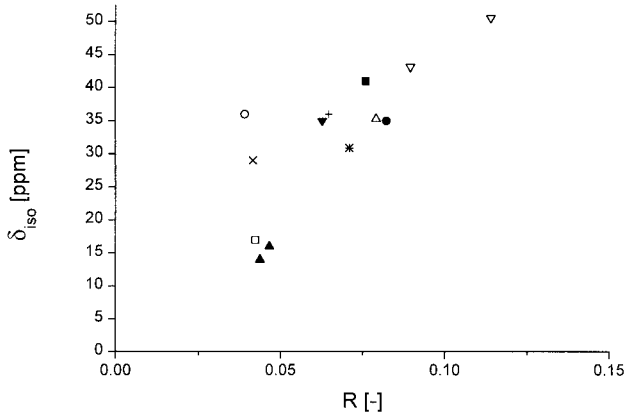

Figure 8. Isotropic chemical shift (δ_{iso}) as a function of the *R* value (eq 5, assuming trigonal bipyramid as ideal shape) of several Al coordinated 5-fold to oxygen. Vesuvianite is not incorporated, because this AlO_5 polyhedron is closest to a tetragonal pyramid shape.[36] Literature: N = NMR data, S = structural data. (□) $SrAl_{12}O_{19}$ (N: this work, S: 2), (*) augelite (N: 12, S: 37), (▲) AlPO-21 (N: 10, S: 38), (○) senegalite (N: 12, S: 39), (▼) $NdAlGeO_7$ (N: 8, S: 40), (+) $Al_2Ge_2O_7$ (N: 8, S: 41), (×) "Pyrophyllite dehydroxylate" (N: 15, S: 42), (●) andulasite (N: 7, S: 43), (■) grandiderite (N: 11,S: 44), (▽) $9Al_2O_3{\cdot}2B_2O_3$ (N: 17, S: 45), (△) $Ba[Al_2(C_2H_4O_2)_4]$ (N: 14, S: 46).

nearest neighbors was established, whereas the distortion of the AlO_4 and AlO_6 polyhedra only influences the observed quadrupole parameters.[6,31,33,47−49]

Comparison of Aluminates with the Magnetoplumbite-Type Structure. The similarities between the ^{27}Al MAS NMR spectra of different aluminates with the magnetoplumbite-type structure were already mentioned in our previous work.[1] This is also clear when the spectra in this work are compared to those published by Müller et al.[5] and Van Hoek et al.[4] These similarities indicate that the influence of the alkali-earth metal in the magnetoplumbites on the NMR parameters is expected to be relatively small. However, the NMR parameters of the Al sites in the magnetoplumbite $CaAl_{12}O_{19}$, as obtained by Müller et al. (shown in parentheses in Table 3),[5] are different from the NMR parameters of the Al sites in the magnetoplumbite $SrAl_{12}O_{19}$, as obtained in the present study.

The principal difference is that the 5-fold-coordinated Al site was not observed in $CaAl_{12}O_{19}$.[5] Independently, Van Hoek et al.[4] expected, based on NMR data of AlO_5 polyhedra published at that time, that the isotropic chemical shift of AlO_5 would be positioned in between the AlO_4 and AlO_6 NMR signals and that the quadrupolar coupling would be very large. It was assumed that the AlO_5 line would be very broad because of the supposed large C_q, which, in combination with the low intensity (only about 8% of the Al atoms occupy this site), would render this site unobservable.[4,5] In the magnetoplumbites (also $CaAl_{12}O_{19}$ and $SrAl_{12}O_{19}$) studied to date the Al ions in the Al(V) site are situated at one crystallographic equivalent position (occupied for 50%).[2,50,51] These positions (with Wyckoff letter 4e) are displaced from the mirror plane, as is shown in Figure 5. This model is called the split atom model.[2,50,51] According to Van Hoek et al., dynamic exchange, instead of statistical disorder, of the aluminum atom between the two equivalent positions of the Al(V) ion results in a dispersion of effective chemical shifts, causing a number of overlapping weak and broadened lines.[4] According to Kimura et al.[2] and Graetsch et al.,[51] such a dynamical order is not possible in $SrAl_{12}O_{19}$ because the equilateral oxygen triangle in the horizontal mirror plane is too small to allow undisturbed vibration of the Al(V) ions through the triangle. In the present study it has been shown that the difficulty in determination of the Al(V) NMR signal is actually caused by the fact that this signal is obscured by the three AlO_6 signals and not due to a large quadrupolar coupling. This site could only be resolved by resorting to MQMAS NMR instead of conventional MAS NMR. This indicates that it is not always possible to directly and unambiguously assign the ^{27}Al NMR signals of 5-fold-coordinated Al in a crystalline material. To enhance the potential of ^{27}Al NMR for solving problems in materials science involving 5-fold-coordinated Al, clearly a better insight into the relation between structural parameters and NMR parameters is needed for AlO_5 polyhedra.

The second difference is that Müller et al. incorrectly determined the NMR parameters for one of the AlO_6 signals (Al(VI)(3), with large quadrupole coupling constant), because only high-field recordings were used.[5] The NMR signal of Al(VI)(3) (with large quadrupole coupling constant) is clearly visible at the low-field recordings of $CaAl_{12}O_{19}$, as shown by Van Hoek et al.[4] The incorrect assignment is a result of the incorrect determination of Al-quadrupole parameters for the Al(VI)(2) and Al(VI)(3) signals reported by Müller et al. (Table 3).[5] The assignments of the NMR signals of the Al(VI)(1) and Al(IV) sites as published by Müller et al. for $CaAl_{12}O_{19}$ are in agreement with the assignments made in this work for $SrAl_{12}O_{19}$.[5] The quadrupole coupling constant of the Al(IV) tetrahedron in $CaAl_{12}O_{19}$ is clearly lower than that in $SrAl_{12}O_{19}$ (2 instead of 3.45 MHz). Indeed, the mean bond angle deviation and the shear strain are lower in $CaAl_{12}O_{19}$ ($D = 2.36$ and $|\psi| = 0.24$ according to structural data[52]) compared to $SrAl_{12}O_{19}$ ($D = 2.60$ and $|\psi| = 0.27$).

Summarizing, it can be stated that the differences in the NMR data as reported by Müller et al.[5] for $CaAl_{12}O_{19}$ and the data presented here for $SrAl_{12}O_{19}$ are partly due to structural differences between these compounds and partly due to some incorrect assignments in the work of Müller et al. The present work clearly shows that (field-dependent) MAS NMR was insufficient to completely assign the spectra. In this particular case we had to resort to 5Q MAS for that purpose.

Conclusions

The first complete assignment and determination of NMR parameters of all crystallographic Al sites, including the 5-fold-coordinated Al, in $SrAl_{12}O_{19}$ was carried out. This compound has the magnetoplumbite structure. Quintuple-quantum (5Q) MAS NMR proved essential to obtain information concerning the quadrupole coupling constant and the isotropic chemical shifts of the various sites, as there are only small differences between these parameters for three of the five Al sites. The simulations of the conventional MAS spectra, recorded at four different magnetic fields, were optimized by taking a small distribution in quadrupole coupling constant into account. The intensities of the isotropic lines were corrected taking the effect of finite spinning speeds into account. These corrected intensities agreed well with the expected intensities.

It is not trivial to unambiguously identify the 5-fold-coordinated Al site based on its ^{27}Al NMR parameters alone when independent evidence is not available. This seems to be a rather general problem that hampers the distinction between 5-fold-coordinated Al sites and other coordinations, especially 6-fold-coordinated sites.

The quadrupole coupling constant of the tetrahedral Al(IV) site in $SrAl_{12}O_{19}$ agrees well with the value expected from the calculated distortion of this tetrahedron. An increasing distortion of the Al octahedra in $SrAl_{12}O_{19}$ results in an increasing quadrupole coupling constant, which is in agreement with literature data concerning this relation for other materials.[31] The

isotropic chemical shift of the trigonal bipyramid AlO_5 site in $SrAl_{12}O_{19}$ is only 18 ppm. This is ascribed to the distortion of the AlO_5 polyhedron; we observed a tentative relationship between the isotropic shift and the distortion parameter *R* defined by Zemann.[35]

Acknowledgment. We thank Mr. J. van Os and Mr. H. Janssen of the SON/NWO HF-NMR Facility (Nijmegen) for their technical support.

References and Notes

(1) Jansen, S. R.; de Haan, J. W.; van de Ven, L. J. M.; Hanssen, R.; Hintzen, H. T.; Metselaar, R. *Chem. Mater.* **1997**, *9*, 1516.
(2) Kimura, K.; Ohgaki, M.; Tanaka, K.; Morikawa, H.; Marumo, F. *J. Solid State Chem.* **1990**, *87*, 186.
(3) Lindop, A. J.; Matthewst, C.; Goodwin, D. W. *Acta Crystallogr. B* **1975**, *31*, 2940.
(4) Van Hoek, J. A. M.; van Loo, F. J. J.; Metselaar, R.; de Haan, J. W.; van den Berg, A. J. *Solid State Ionics* **1991**, *45*, 93.
(5) Müller, D.; Gessner, W.; Samoson, A.; Lippmaa, E.; Scheler, G. *Polyhedron* **1986**, *5*, 779.
(6) Smith, M. E. *Appl. Magn. Reson.* **1993**, *4*, 1.
(7) Alemany, L. B.; Massiot, D.; Sherrif, B. L.; Smith, M. E.; Taulelle, F. *Chem. Phys. Lett.* **1991**, *177*, 301.
(8) Massiot, D.; Kahn-Harari, A.; Michel, D.; Müller, D.; Taulelle, F. *Magn. Reson. Chem.* **1990**, *28*, S82.
(9) Alemany, L. B.; Timken, H. K. C.; Johnson, I. D. *J. Magn. Reson.* **1988**, *80*, 427.
(10) Jelinek, R.; Chmelka, B. F.; Wu, Y.; Grandinetti, P. J.; Pines, A.; Barrie, P. J.; Klinowski, J. *J. Am. Chem. Soc.* **1991**, *113*, 4097.
(11) Smith, M. E.; Steuernagel, S. *Solid State NMR* **1992**, *1*, 175.
(12) Bleam, W. F.; Dec, S. F.; Frye, J. S. *Phys. Chem. Miner.* **1987**, *16*, 817.
(13) Phillips, B. L.; Allen, F. M.; Kirkpatrick, R. *J. Am. Mineral.* **1987**, *72*, 1190.
(14) Cruickshank, M. C.; Glasser, L. S. D.; Barrie, S. A. I.; Poplett, I. J. F. *J. Chem. Soc., Chem. Commun.* **1986**, *88*, 23.
(15) Fitzgerald, J. J.; Dec, S. F.; Hamza, A. I. *Am. Mineral.* **1989**, *74*, 1405.
(16) Kunath, G.; Losso, P.; Steuernagel, S.; Schneider, H.; Jäger, C. *Solid State NMR* **1992**, *1*, 261.
(17) Massiot, D.; Müller, D.; Hübert, T.; Schneider, M.; Kentgens, A. P. M.; Coté, B.; Coutures, J. P.; Gessner, W. *Solid State NMR* **1995**, *5*, 175.
(18) Samoson, A.; Lippmaa, E.; Pines, A. *Mol. Phys.* **1988**, *65*, 1013.
(19) Llor, A.; Virlet, J. *J. Chem. Phys. Lett.* **1988**, *152*, 248.
(20) Mueller, K. T.; Sun, B. Q.; Chingas, G. C.; Zwanziger, J. W.; Terao, T.; Pines, A. *J. Magn. Reson.* **1990**, *86*, 470.
(21) Frydman, L.; Harwood, J. S. *J. Am. Chem. Soc.* **1995**, *117*, 5367.
(22) Medek, A.; Harwood, J. S.; Frydman, L. *J. Am. Chem. Soc.* **1995**, *117*, 12779.
(23) Fernandez, C.; Amoureux, J. P. *Chem. Phys. Lett.* **1995**, *242*, 449.
(24) Jansen, S. R.; Hintzen, H. T.; Metselaar, R. *Fourth Euro-Ceramics. Basic Science−Developments in processing of advanced ceramics−part II*; Gruppo Editoriale Faenza Editrice S.p.A.: Italy, 1995; p 353.
(25) Amoureux, J. P.; Fernandez, C.; and Steuernagel, S. *J. Magn. Reson. A.* **1996**, *123*, 116.
(26) Winfit 950425, Bruker-Franzen Analytik GmbH, 1995.
(27) Baltisberger, J. H.; Xu, Z.; Stebbins, J. F.; Wang, S. H.; Pines, A. *J. Am. Chem. Soc.* **1996**, *118*, 7209.
(28) Kentgens, A. P. M. Matlab simulation.
(29) Massiot, D.; Bessada, C.; Coutures, J. P.; Taulelle, F. *J. Magn. Reson.* **1990**, *90*, 231.
(30) Skibsted, J.; Henderson, B.; Jakobsen, H. J. *Inorg. Chem.* **1993**, *32*, 1013.
(31) Ghose, S., Tsang, T. *Am. Mineral.* **1973**, *58*, 748.
(32) Engelhardt, G., Veeman, W. *J. Chem. Soc., Chem. Commun.* **1993**, 622.
(33) Peeters, M. P. J.; Van de Ven, L. J. M.; De Haan, J. W.; Van Hooff, J. H. C. *J. Phys. Chem.* **1993**, *97*, 5563.
(34) Müller, D.; Gessner, W.; Samoson, A.; Lippmaa, E.; Scheler, G. *J. Chem. Soc., Dalton Trans.* **1986**, 1277.
(35) Zemann, J. *Z. Anorg. Allg. Chem.* **1963**, *324*, 241.
(36) Yoshiasa, A., Matsumoto, T. *Miner. J.* **1986**, *13*, 1.
(37) Pearson, W. B.; Shoemaker, C. B.; Duckworth, V. Structure reports. Volume 33A. Oosthoek, Scheltema & Holkema: Urecht, 1968, p 403.
(38) Bennet, J. M.; Cohen, J. M.; Artiali, G.; Pluth, J. J.; Smith, J. V. *Inorg. Chem.* **1985**, *24*, 188.
(39) Keegan, T. D.; Araki, T.; Moore, P. B. *Am. Mineral.* **1979**, *64*, 1243.
(40) Jarchow, O.; Klaska, K.-H. *Z. Kristall.* **1985**, *172*, 159.
(41) Agafonov, V.; Kahn, A.; Michel, D.; Perez y Jorba, M. *J. Solid State Chem.* **1986**, *62*, 402.
(42) Wardle, R.; Brindley, G. W. *Am. Mineral.* **1972**, *57*, 732.
(43) Burnham, C. W.; Buerger, M. J. *Z. Kristall.* **1961**, *115*, 269.
(44) Stephenson, D. A.; Moore, P. B. *Acta Crystallogr. B* **1968**, *24*, 1518.
(45) Garsche, M.; Tillmanns, E.; Almen, H.; Schneider, H.; Kupcik, V. *Eur. J. Mineral.* **1991**, *3*, 793.
(46) Cruickshank, M. C.; Glasser, L. S. D. *Acta Crystallogr. C* **1985**, *41*, 1014.
(47) Lippmaa, E.; Samoson, A.; Mägi, M. *J. Am. Chem. Soc.* **1986**, *108*, 1730.
(48) Müller, D.; Jahn, E.; Ladwig, G.; Haubenreisser, U. *Chem. Phys. Lett.* **1984**, *109*, 332.
(49) Jacobsen, H. S.; Norby, P.; Bildsoe, H.; Jakobsen, H. J. *Zeolites* **1989**, *9*, 491.
(50) Graetsch, H.; Gebert, W. Z. *Kristall.* **1995**, *210*, 9.
(51) Graetsch, H.; Gebert, W. Z. *Kristall.* **1994**, *209*, 338.
(52) Utsunomiya, A.; Tanaka, K.; Morikawa, H.; Marumo, F.; Kojima, H. *J. Solid State Chem.* **1988**, *75*, 197.